This paper is published as part of a PCCP Themed Issue on:
Time-Dependent Density-Functional Theory

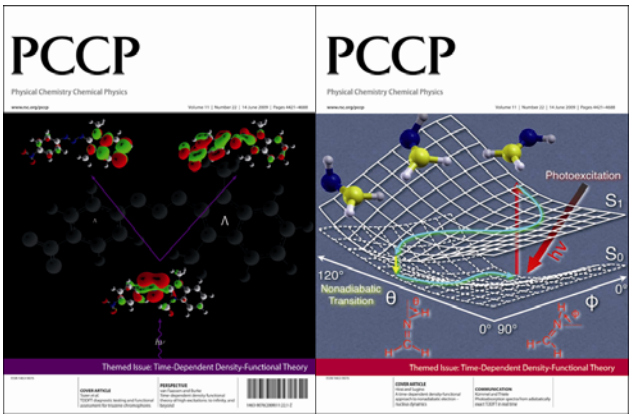

Guest Editors:

Miguel A. L. Marques and Angel Rubio

Editorial

Time-dependent density-functional theory
Phys. Chem. Chem. Phys., 2009
DOI: 10.1039/b908105b

Perspective

Time-dependent density functional theory of high excitations: to infinity, and beyond
Meta van Faassen and Kieron Burke, *Phys. Chem. Chem. Phys.*, 2009
DOI: 10.1039/b901402k

Papers

Time-dependent density functional theory *versus* Bethe–Salpeter equation: an all-electron study
Stephan Sagmeister and Claudia Ambrosch-Draxl, *Phys. Chem. Chem. Phys.*, 2009
DOI: 10.1039/b903676h

TD-DFT calculations of electronic spectra of hydrogenated protonated polycyclic aromatic hydrocarbon (PAH) molecules: implications for the origin of the diffuse interstellar bands?
Mark Hammonds, Amit Pathak and Peter J. Sarre, *Phys. Chem. Chem. Phys.*, 2009
DOI: 10.1039/b903237a

TDDFT diagnostic testing and functional assessment for triazene chromophores
Michael J. G. Peach, C. Ruth Le Sueur, Kenneth Ruud, Maxime Guillaume and David J. Tozer, *Phys. Chem. Chem. Phys.*, 2009
DOI: 10.1039/b822941d

An *ab initio* and TD-DFT study of solvent effect contributions to the electronic spectrum of Nile Red
Patrick Owen Tuck, Robert Christopher Mawhinney and Manit Rappon, *Phys. Chem. Chem. Phys.*, 2009
DOI: 10.1039/b902528f

Towards a gauge invariant method for molecular chiroptical properties in TDDFT
Daniele Varsano, Leonardo A. Espinosa-Leal, Xavier Andrade, Miguel A. L. Marques, Rosa di Felice and Angel Rubio, *Phys. Chem. Chem. Phys.*, 2009
DOI: 10.1039/b903200b

Second-order nonlinear optical properties of transition metal clusters [$MoS_4Cu_4X_2Py_2$] (M = Mo, W; X = Br, I)
Qiaohong Li, Kechen Wu, Yongqin Wei, Rongjian Sa, Yiping Cui, Canggui Lu, Jing Zhu and Jiangang He, *Phys. Chem. Chem. Phys.*, 2009
DOI: 10.1039/b903582f

Absorption and fluorescence properties of oligothiophene biomarkers from long-range-corrected time-dependent density functional theory
Bryan M. Wong, Manuel Piacenza and Fabio Della Sala, *Phys. Chem. Chem. Phys.*, 2009
DOI: 10.1039/b901743g

Time-dependent current-density functional theory for generalized open quantum systems
Joel Yuen-Zhou, César Rodríguez-Rosario and Alán Aspuru-Guzik, *Phys. Chem. Chem. Phys.*, 2009
DOI: 10.1039/b903064f

Optical and magnetic properties of boron fullerenes
Silvana Botti, Alberto Castro, Nektarios N. Lathiotakis, Xavier Andrade and Miguel A. L. Marques, *Phys. Chem. Chem. Phys.*, 2009
DOI: 10.1039/b902278c

Inhomogeneous STLS theory and TDCDFT
John F. Dobson, *Phys. Chem. Chem. Phys.*, 2009
DOI: 10.1039/b904385n

Bound states in time-dependent quantum transport: oscillations and memory effects in current and density
E. Khosravi, G. Stefanucci, S. Kurth and E.K.U. Gross, *Phys. Chem. Chem. Phys.*, 2009
DOI: 10.1039/b906528h

Time-dependent density functional theory for resonant properties: resonance enhanced Raman scattering from the complex electric-dipole polarizability
Abdelsalam Mohammed, Hans Ågren and Patrick Norman, *Phys. Chem. Chem. Phys.*, 2009
DOI: 10.1039/b903250a

On the proton transfer mechanism in ammonia-bridged 7-hydroxyquinoline: a TDDFT molecular dynamics study
Matteo Guglielmi, Ivano Tavernelli and Ursula Rothlisberger, *Phys. Chem. Chem. Phys.*, 2009
DOI: 10.1039/b903136g

Chemical and protein shifts in the spectrum of the photoactive yellow protein: a time-dependent density functional theory/molecular mechanics study
Eneritz Muguruza González, Leonardo Guidoni and Carla Molteni, *Phys. Chem. Chem. Phys.*, 2009
DOI: 10.1039/b902615k

Excitation energies from ground-state density-functionals by means of generator coordinates
E. Orestes, A. B. F. da Silva and K. Capelle, *Phys. Chem. Chem. Phys.*, 2009
DOI: 10.1039/b902529d

A time-dependent density-functional approach to nonadiabatic electron-nucleus dynamics: formulation and photochemical application
Hirotoshi Hirai and Osamu Sugino, *Phys. Chem. Chem. Phys.*, 2009
DOI: 10.1039/b901144g

Wavepacket basis for time-dependent processes and its application to relaxation in resonant electronic transport
Peter Bokes, *Phys. Chem. Chem. Phys.*, 2009
DOI: 10.1039/b902501d

Can phthalocyanines and their substituted α-*para*-(methoxy)phenyl derivatives act as photosensitizers in photodynamic therapy? A TD-DFT study
Angelo Domenico Quartarolo, Ida Lanzo, Emilia Sicilia and Nino Russo, *Phys. Chem. Chem. Phys.*, 2009
DOI: 10.1039/b819064j

Substituent effects on the light-induced C–C and C–Br bond activation in (bisphosphine)(η^2-tolane)Pt^0 complexes. A TD-DFT study
Daniel Escudero, Mariana Assmann, Anne Pospiech, Wolfgang Weigand and Leticia González, *Phys. Chem. Chem. Phys.*, 2009
DOI: 10.1039/b903603b

Photodegradation mechanism of the common non-steroid anti-inflammatory drug diclofenac and its carbazole photoproduct
Klefah A. K. Musa and Leif A. Eriksson, *Phys. Chem. Chem. Phys.*, 2009
DOI: 10.1039/b900144a

Computation of accurate excitation energies for large organic molecules with double-hybrid density functionals
Lars Goerigk, Jonas Moellmann and Stefan Grimme, *Phys. Chem. Chem. Phys.*, 2009
DOI: 10.1039/b902315a

Time-dependent current density functional theory *via* time-dependent deformation functional theory: a constrained search formulation in the time domain
I. V. Tokatly, *Phys. Chem. Chem. Phys.*, 2009
DOI: 10.1039/b903666k

Photoabsorption spectra from adiabatically exact time-dependent density-functional theory in real time
Mark Thiele and Stephan Kümmel, *Phys. Chem. Chem. Phys.*, 2009
DOI: 10.1039/b902567g

Double excitation effect in non-adiabatic time-dependent density functional theory with an analytic construction of the exchange–correlation kernel in the common energy denominator approximation
Oleg V. Gritsenko and Evert Jan Baerends, *Phys. Chem. Chem. Phys.*, 2009
DOI: 10.1039/b903123e

Physical signatures of discontinuities of the time-dependent exchange–correlation potential
Daniel Vieira, K. Capelle and C. A. Ullrich, *Phys. Chem. Chem. Phys.*, 2009
DOI: 10.1039/b902613d

Autoionizing resonances in time-dependent density functional theory
August J. Krueger and Neepa T. Maitra, *Phys. Chem. Chem. Phys.*, 2009
DOI: 10.1039/b902787d

The polarizability in solution of tetra-phenyl-porphyrin derivatives in their excited electronic states: a PCM/TD-DFT study
Roberto Improta, Camilla Ferrante, Renato Bozio and Vincenzo Barone, *Phys. Chem. Chem. Phys.*, 2009
DOI: 10.1039/b902521a

A new generalized Kohn–Sham method for fundamental band-gaps in solids
Helen R. Eisenberg and Roi Baer, *Phys. Chem. Chem. Phys.*, 2009
DOI: 10.1039/b902589h

Bound states in time-dependent quantum transport: oscillations and memory effects in current and density

E. Khosravi,[ab] G. Stefanucci,[cb] S. Kurth[db] and E. K. U. Gross[ab]

Received 1st April 2009, Accepted 29th April 2009
First published as an Advance Article on the web 11th May 2009
DOI: 10.1039/b906528h

The presence of bound states in a nanoscale electronic system attached to two biased, macroscopic electrodes is shown to give rise to persistent, non-decaying, localized current oscillations which can be much larger than the steady part of the current. The amplitude of these current oscillations and of the corresponding density oscillations depends on the entire history of the applied potential. The bound-state contribution to the time-averaged density turns out to be history-dependent as well and leads to a natural definition of the bound-state occupations out of equilibrium.

In recent years it has become possible to measure the current through single molecules attached to two macroscopic electrodes.[1,2] This is hoped to be a first step towards the vision of "molecular electronics" where single molecules become the basic units (transistors, *etc*.) of highly miniaturized electronic devices.

To address electronic transport on such a small scale theoretically, one needs a full quantum description of the electronic dynamics. Non-equilibrium Green's functions (NEGF) provide a natural framework to study quantum transport properties of nanoscale devices coupled to leads. When a bias is applied, the electrodes remain in local equilibrium while the current is driven by the different chemical potentials in the left and right lead. In model systems the leads are assumed to be non-interacting and the current is computed from the Meir–Wingreen formula[3] using approximate many-body self-energies $\Sigma_{\rm MB}$. For weakly correlated models $\Sigma_{\rm MB} \sim 0$ and the Meir–Wingreen formula reduces to the Landauer– Büttiker formula,[4,5] as it should.

If one wants to account for the full atomistic structure of the system, the NEGF formalism is usually combined with static density functional theory (DFT) and the current is computed from a Landauer-type equation.[6–14] This approach enjoys increasing popularity, in particular for the description of transport experiments on single molecules.[1] From a fundamental point of view, however, the use of static DFT—which is an equilibrium theory—is not justified to describe non-equilibrium situations. For a critical review of this methodology, the reader is referred to ref. 15.

By construction, the NEGF + DFT approach inherits the main assumption of the Landauer formalism that for a system driven out of equilibrium by a dc bias, a steady current will eventually develop. In other words, the dynamical formation of a steady state does not follow from the formalism but rather constitutes an assumption. The question of how the system reaches the steady state has been addressed theoretically in ref. 16 & 17 where it was shown that the total current (and the density) reaches a steady value if the local density of states is a smooth function of energy in the device region. In the same work it was also shown that for non-interacting electrons the steady current is independent both of the initial conditions and of the history of the bias, *i.e*., all memory effects are washed out.

The situation is different, however, if there exist two or more localized bound states (BS) in the device region, *i.e*., if the local density of states has sharp peaks at certain energies. In this case a non-interacting system exposed to a dc bias *does not* evolve to a steady state.[18–20]

Let $\boldsymbol{H}^0$ be the one-particle Hamiltonian of the system in equilibrium. At positive times we perturb the system with a longitudinal electric field and we assume that the one-particle Hamiltonian $\boldsymbol{H}(t)$ globally converges to a time-independent Hamiltonian $\boldsymbol{H}^\infty$ when $t \to \infty$. We further assume that for any two points $\boldsymbol{r}$ and $\boldsymbol{r}'$ in electrode α the quantity $\langle \boldsymbol{r}'|\boldsymbol{H}(t)-\boldsymbol{H}^0|\boldsymbol{r}\rangle = U_\alpha(t)\delta(\boldsymbol{r}-\boldsymbol{r}')$ where $|\boldsymbol{r}\rangle$ is a position eigenket and $U_\alpha(t)$ is a spatially uniform, time-dependent shift. In that case, the unitary operator (atomic units are used throughout)

$$M^\dagger = \lim_{t\to\infty} e^{i\boldsymbol{H}^\infty t}\,\mathcal{T}[e^{-i\int_0^t d\tau \boldsymbol{H}(\tau)}], \qquad (1)$$

with $\mathcal{T}$ being the time-ordering operator, is well defined and we can express the one-particle density matrix $\rho(\boldsymbol{r},\boldsymbol{r}';t)$ in the long-time limit as

$$\rho(\boldsymbol{r},\boldsymbol{r}';t\to\infty) = \langle \boldsymbol{r}|e^{-i\boldsymbol{H}^\infty t}\boldsymbol{M}^\dagger f(\boldsymbol{H}^0)\boldsymbol{M}e^{i\boldsymbol{H}^\infty t}|\boldsymbol{r}'\rangle, \qquad (2)$$

where $f(\boldsymbol{H}^0)$ is the Fermi function with argument $\boldsymbol{H}^0$. Let $|\psi_b\rangle$ be the bound eigenstates of $\boldsymbol{H}^\infty$ with eigenenergies ε_b and $|\psi_k\rangle$ the continuum eigenstates of $\boldsymbol{H}^\infty$ with eigenenergies ε_k. Inserting twice the completeness relation $1 = \Sigma_b |\psi_b\rangle\langle\psi_b| + \Sigma_k |\psi_k\rangle\langle\psi_k|$ one can rewrite eqn (2) as

$$\rho(\boldsymbol{r},\boldsymbol{r}';t\to\infty) = \sum_{b,b'} \psi_b(\boldsymbol{r}) f_{b,b'} \psi^*_{b'}(\boldsymbol{r}') e^{-i(\varepsilon_b-\varepsilon_{b'})t} + \sum_k \psi_k(\boldsymbol{r}) f_{k,k} \psi^*_k(\boldsymbol{r}'), \qquad (3)$$

[a] *Institut für Theoretische Physik, Freie Universität Berlin, Arnimallee 14, D-14195 Berlin, Germany*
[b] *European Theoretical Spectroscopy Facility (ETSF), Europe*
[c] *Department of Physics, University of Rome Tor Vergata, Via della Ricerca Scientifica 1, 00133 Rome, Italy*
[d] *Nano-Bio Spectroscopy Group, Dpto. de Física de Materiales, Universidad del País Vasco UPV/EHU, Centro Mixto CSIC-UPV/EHU, Av. Tolosa 72, E-20018 San Sebastián, Spain*

with

$$f_{b,b'} = \langle\psi_b|\boldsymbol{M}^\dagger f(\boldsymbol{H}^0)\boldsymbol{M}|\psi_{b'}\rangle \quad (4)$$

and $f_{k,k} = \langle\psi_b|\boldsymbol{M}^\dagger f(\boldsymbol{H}^0)\boldsymbol{M}|\psi_k\rangle$. In eqn (3) we have used the Riemann–Lebesgue theorem to cancel the bound-continuum contributions and the off-diagonal terms of the continuum-continuum contribution.[19] Clearly, by virtue of eqn (1), the operator $\boldsymbol{M}$ depends on the history of the time-dependent perturbation. Therefore the coefficients $f_{b,b'}$ are matrix elements of $f(\boldsymbol{H}^0)$ between history-dependent localized functions.

In eqn (3) a steady component of ρ is superimposed by undamped harmonic oscillations. The total current through a plane Π perpendicular to the transport geometry has the form

$$\lim_{t\to\infty} I_\Pi(t) = I_\Pi^{(S)} + I_\Pi^{(D)}(t), \quad (5)$$

where the steady contribution $I_\Pi^{(S)}$ is given by the Landauer formula. The dynamical part, $I_\Pi^{(D)}(t)$, reads

$$I_\Pi^{(D)}(t) = 2\sum_{b,b'} f_{b,b'}\Lambda_{b,b'}^\Pi \sin[(\varepsilon_b - \varepsilon_{b'})t], \quad (6)$$

where

$$\Lambda_{b,b'}^\Pi = \int_\Pi \mathrm{d}\sigma\ \hat{\mathbf{n}}\cdot\psi_{b'}^*(\boldsymbol{r})\nabla\psi_b(\boldsymbol{r}). \quad (7)$$

In eqn (7) the surface integral is over the plane Π and $\hat{\mathbf{n}}$ is the unit vector perpendicular to the surface element $\mathrm{d}\sigma$. It is worth noting that the operator $\boldsymbol{M}$, which we will call "memory operator" from now on, appears in both quantities $I_\Pi^{(S)}$ and $I_\Pi^{(D)}$ through the coefficients $f_{k,k}$ and $f_{b,b'}$. In the steady part, however, the history dependence cancels out.[19] The question whether or not history dependent effects can actually be observed in the dynamical contribution, $I_\Pi^{(D)}(t)$, is one of the central issues addressed below.

In the present work we demonstrate by numerical simulations that (i) the amplitude of the current oscillations may be very large compared to the steady component of the current; (ii) the amplitude of the current oscillations may be strongly history dependent; (iii) our time-dependent approach provides a natural way to properly define the occupation numbers of BS with energies in the bias window. It should be remembered that within the standard NEGF + DFT approach, the question of how to take BS into account in the calculation of the density[11,22] has, so far, remained an unsolved problem. Here we show how the BS occupations naturally result from the time evolution of the underlying time dependent Kohn–Sham (TDKS) system; and (iv) we demonstrate the intuitively
expected result that the BS occupations are history-dependent, *i.e.*, they depend on how the potential is switched on.

In order to investigate in detail the actual dependence of the coefficients $f_{b,b'}$ on the history of the TD perturbation, we study model systems of non-interacting electrons at zero temperature using a recently proposed algorithm[21] suitable to describe TD transport through open systems. The central feature of this algorithm is that it allows for the numerically exact solution of the TD Schrödinger equation in the central device region in the presence of the semi-infinite electrodes. We consider one-dimensional systems described by the TD Hamiltonian

$$H(x,t) = -\frac{1}{2}\frac{\mathrm{d}^2}{\mathrm{d}x^2} + U_0(x) + U(x,t). \quad (8)$$

For times $t < 0$ the system is in its ground state described by the Hamiltonian $H^0(x) = -\frac{\nabla^2}{2} + U_0(x)$. At $t = 0$ the system is driven out of equilibrium by applying a TD field $U(x,t)$. We choose the TD perturbation in such a way that for $t \to \infty$ the Hamiltonian globally converges to an asymptotic Hamiltonian, $H^\infty(x)$.

The TD perturbation can be split into three sub-regions depending on where in the system it is imposed: U_α with $\alpha = L,R$, represents the applied bias in the left (L) and right (R) leads and is independent of the position within the lead. In the central region, the TD perturbation (which we call a gate voltage $V_g(x,t)$) may depend both on position x and time t. Thus, the total TD perturbation can be written as

$$U(x,t) = \begin{cases} U_\mathrm{L}(t) & -\infty < x < x_\mathrm{L} \\ V_g(x,t) & x_L < x < x_\mathrm{R} \\ U_\mathrm{R}(t) & x_\mathrm{R} < x < \infty \end{cases}. \quad (9)$$

In the numerical simulations described below, the explicit propagation window ranges from $x_\mathrm{L} = -1.2$ a.u. to $x_\mathrm{R} = 1.2$ a.u. We choose a lattice spacing $\Delta x = 0.012$ a.u. and use a simple three-point discretization for the kinetic energy. The initial potential is $U_0(x) = 0$ for any point x in the left or right lead. Therefore, the occupied part of the continuous spectrum ranges from momenta $k = -k_\mathrm{F} = -\sqrt{2\varepsilon_\mathrm{F}}$ to $k = k_\mathrm{F}$ which is discretized with 400 k-points (ε_F being the Fermi energy). The (non-interacting) many-body state is propagated from $t = 0$ to $t = 1400$ a.u. using a time step $\Delta t = 0.05$ a.u.

In the first model the initial state is a Slater determinant of plane waves with energies less than $\varepsilon_\mathrm{F} = 0.1$ a.u. At $t = 0$ we suddenly switch on a bias $U_\mathrm{L} = 0.15$ a.u. in the left lead and as a result a current flows which after some transient time reaches a steady value of about 0.027 a.u. After the steady state is attained, at time $T = 100$ a.u., we switch on a gate potential

$$V_\mathrm{g}(x,t) = -\frac{(t-T)}{T_\mathrm{g}}v_\mathrm{g} \quad (10)$$

for $T < t < T + T_\mathrm{g}$ with a switching time $T_\mathrm{g} = 20$ a.u. and the final depth of the potential well $v_g = 1.3$ a.u. For times $t \geq T + T_\mathrm{g}$ this gate potential remains unchanged at $V_g(x,t) = -v_g$ and supports two BS at $\varepsilon_1 = -0.933$ a.u. and $\varepsilon_2 = -0.063$ a.u.

The resulting TD current in the center of the device region is shown in the upper left panel of Fig. 1. The development of a steady-state current for $T < 100$ a.u. can clearly be recognized. After the BS are created ($t > T + T_\mathrm{g}$) the current starts to oscillate as expected. The amplitude of the current oscillation is of the order of 0.35 a.u., *i.e.*, more than an order magnitude larger than the steady-state current.

The history dependence of the current oscillations can be seen by comparing the current in the upper and lower left panels of Fig. 1. Both currents were computed by starting from the same initial state and applying the same bias at $t = 0$. In the lower panel we create the same, final potential as in the upper panel, but in two steps. At $T = 100$ a.u. we suddenly

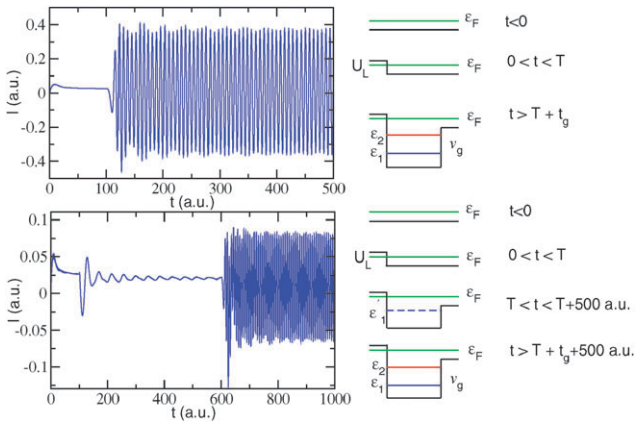

Fig. 1 Time evolution of the current at $x = 0$. At $t = 0$ a.u., a bias $U_L = 0.15$ a.u. is suddenly switched on and the system evolves to a steady state. Upper panels: at $T = 100$ a.u., a gate potential is turned on ($v_g = 1.3$ a.u. and $T_g = 20$ a.u.) which creates two BS and results in large amplitude oscillations of the current. A sequence of the time-dependent potential is sketched in the right panel. Lower panels: at $T = 100$ a.u., a first gate potential ($v_g = 0.2$ a.u. and $T_g = 0$) is turned on which creates a single BS. Waiting for the transients to decay, a second gate voltage ($v_g = 1.1$ a.u. and $T_g = 20$ a.u.) is then applied which leads to the formation of a second BS and therefore to persistent current oscillations (again, the right panel sketches the potential sequence). Although $\boldsymbol{H}^{\infty}$ is identical in both cases, the amplitude of the current oscillation is significantly smaller in the second case, illustrating its dependence on the history of the system.

switch on a first gate potential with depth $v_g = 0.2$ a.u. which creates only one BS. Waiting for the slow decay of the resulting bound-continuum transitions we then apply an additional gate potential of depth $v_g = 1.1$ a.u. (hence the total depth is 1.3 a.u.) with a switching time $T_g = 20$ a.u. Again we recognize the persistent current oscillations due to the bound–bound transition. Although the amplitude (about 0.07 a.u.) is still large compared to the steady-state current, it is about a factor of four smaller than the amplitude in the previous case.

Clearly, BS oscillations not only appear in the current but also in the density, because current and density oscillations are connected through the continuity equation. As a consequence we observe memory effects in the amplitude of the density oscillations as well.

By eqn (5), the current consists of the steady-state (Landauer) part , $I_{\Pi}^{(S)}$, and the dynamic part, $I_{\Pi}^{(D)}(t)$. Correspondingly, the density has a steady-state part and a dynamical contribution. The latter is given by

$$n^{(D)}(\boldsymbol{r}, t) = \sum_{b,b'} f_{b,b'} \cos[(\varepsilon_b - \varepsilon_{b'})t] \psi_{b'}^{*}(\boldsymbol{r}) \psi_b(\boldsymbol{r}). \qquad (11)$$

Interestingly, in contrast to the dynamical current, the dynamical density $n^{(D)}(\boldsymbol{r},t)$ contains a time-independent part arising from the diagonal ($b = b'$) contributions to the double sum in eqn (11). It is exactly this fact that allows us to interpret the coefficients $f_{b,b}$ as occupation numbers of the BS in the long-time limit. Thus, the TD description provides a natural solution to the problem of how to populate BS in transport calculations. In the standard NEGF + DFT approach, BS below the bias window are entirely populated (*i.e.*, $f_{b,b} = 1$) while BS within the bias window are populated empirically with some plausible choice[23] of occupation numbers. Of course, due to its self-consistent nature, the solution of the NEGF + DFT approach is affected by this somewhat arbitrary choice of BS occupations.

To illustrate the existence of memory effects in the time-independent part of the density we have computed $n_{av}(x)$, the time-dependent density averaged over an oscillation period for a system with two bound states in the final Hamiltonian. The system is the one which leads to the current shown in the upper left panel of Fig. 1 except that the gate potential is turned on with different switching times T_g. In Fig. 2 we show $n_{av}(x)$ for three different values of T_g and, as one can see, the corresponding $n_{av}(x)$ differ quite substantially. This difference has to be attributed to BS since for the contribution of the scattering states all memory is washed out.[17] Of course, the relative importance of the BS contribution to $n_{av}(x)$ will decrease when ε_F (and therefore the contribution of the continuum states) increases. By subtracting the continuum contribution from n_{av} and fitting the explicit function $n^{(D)}$ with the numerical curve (where the only fitting parameters are the coefficients $f_{b,b}$ for $b = 1,2$) we have been able to calculate the BS occupations $f_{b,b}$. Those are shown in the inset of Fig. 2 as a function of T_g. Remarkably we find that $f_{b,b}$ exhibits rather large deviations from unity, especially for small switching times. In other words, choosing full occupation ($f_{b,b} = 1$) for the bound states below the bias window is justified only for the case of adiabatic switching. As one would intuitively expect, the occupation of the state with lower energy ($b = 1$) is larger than for the state with higher energy. In the adiabatic limit of very slow switching ($T_g \to \infty$), both occupation numbers approach unity which is expected since both states are energetically below ε_F. The occupation numbers also offer an intuitive qualitative picture of the size of the current and density oscillations: for relatively short switching times ($T_g \leq 50$ a.u.) the occupation

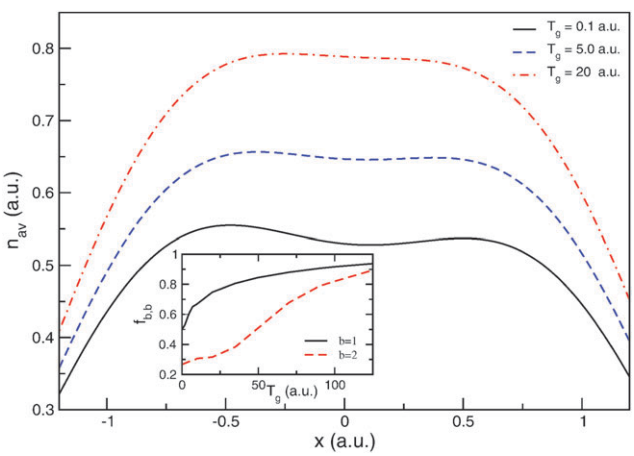

Fig. 2 Memory effects for the static part of the density in the long-time limit in the presence of BS. The densities shown here correspond to systems studied in the upper panel of Fig. 1 except that they are computed for three different switching times of the gate potential of eqn (10): $T_g = 0.1$ a.u. (solid line), $T_g = 5.0$ a.u. (dashed), and $T_g = 20$ a.u. (dash-dotted). The inset shows the occupation numbers $f_{b,b}$ (eqn (4)) of the two bound states as function of switching time.

numbers deviate substantially from one. Therefore the transition probability between the bound states is relatively large and so are the oscillations in current and density. On the other hand, for large switching times both bound states are almost "fully" occupied and the probability of a transition between them is small, leading to small amplitudes in the dynamical density.

In summary we have demonstrated that: (1) the persistent current oscillations in the presence of BS can be much larger than the steady-state current; (2) the amplitude of the current oscillations can have a strong dependence on the history of the system; (3) a similar history dependence is found for the contribution of the BS to the density; and (4) the occupation of BS below and within the bias window is well-defined in a TD description of quantum transport. We would like to emphasize the importance of these results for all transport calculations: the first three points challenge one of the fundamental assumptions of the Landauer formalism (the assumption that a unique steady state always develops) while the fourth point solves the problem of properly defining the BS occupations. Hence the TD approach to transport provides a natural, unified framework to describe current oscillations, memory effects and BS occupations.

In the simulations presented above, electron–electron and electron–phonon interactions have not been included. In real systems, of course, electron–phonon scattering leads to a level broadening and hence damping of the oscillations with a typical time scale of picoseconds. However, since ultimately one wants to exploit the ability of molecular electronics devices to switch on the electronic time scale (femtoseconds), phononic damping is less important while the BS oscillations become extremely relevant. To assess the role of the electron–electron interaction, we point out that the entire formalism remains valid for any effective single-particle theory such as, *e.g.*, TD Hartree–Fock (which treats interactions approximately) or TDDFT (which can treat interactions in principle exactly). In these kind of theories, essentially two situations are conceivable: in the first scenario the effective single-particle potential converges to a time-independent potential, supporting bound states in the long-time limit. If this approach is sufficiently fast then, by eqn (5), oscillating currents will appear. In the second scenario, the effective single-particle potentials are time-dependent (with the BS eigenenergy differences as prominent frequencies) leading again to time-dependent currents and densities (by virtue of Floquet's theorem). This is evidently achieved in approximations such as adiabatic LDA. Although this argument is clearly not mathematically rigorous, the in-principle exact single-particle nature of the TDKS equations suggests that even in the presence of electron–electron interactions oscillations may appear.

We gratefully acknowledge financial support by the Deutsche Forschungsgemeinschaft through the SFB 658. S. K. acknowledges support through the Ikerbasque foundation.

References

1 M. A. Reed, C. Zhou, C. J. Muller, T. P. Burgin and J. M. Tour, *Science*, 1997, **278**, 252.
2 A. I. Yanson, G. Rubio Bollinger, H. E. van den Brom, N. Agraït and J. M. van Ruitenbeek, *Nature*, 1998, **395**, 783.
3 Y. Meir and N. S. Wingreen, *Phys. Rev. Lett.*, 1992, **68**, 2512.
4 R. Landauer, *IBM J. Res. Dev.*, 1957, **1**, 233.
5 M. Büttiker, *Phys. Rev. Lett.*, 1986, **57**, 1761.
6 N. D. Lang, *Phys. Rev. B: Condens. Matter Mater. Phys.*, 1995, **52**, 5335.
7 K. Hirose and M. Tsukada, *Phys. Rev. B: Condens. Matter Mater. Phys.*, 1995, **51**, 5278.
8 J. M. Seminario, A. G. Zacarias and J. M. Tour, *J. Am. Chem. Soc.*, 1998, **120**, 3970.
9 J. Taylor, H. Guo and J. Wang, *Phys. Rev. B: Condens. Matter Mater. Phys.*, 2001, **63**, 245407.
10 J. J. Palacios, A. J. Pérez-Jiménez, E. Louis and J. Vergés, *Phys. Rev. B: Condens. Matter Mater. Phys.*, 2001, **64**, 115411.
11 Y. Xue, S. Datta and M. A. Ratner, *Chem. Phys.*, 2002, **281**, 151.
12 M. Brandbyge, J.-L. Mozos, P. Ordejón, J. Taylor and K. Stokbro, *Phys. Rev. B: Condens. Matter Mater. Phys.*, 2002, **65**, 165401.
13 F. Evers, F. Weigend and M. Koentopp, *Phys. Rev. B: Condens. Matter Mater. Phys.*, 2004, **69**, 235411.
14 S. V. Faleev, F. Leonard, D. A. Stewart and M. van Schilfgaarde, *Phys. Rev. B: Condens. Matter Mater. Phys.*, 2005, **71**, 195422.
15 M. Koentopp, C. Chang, K. Burke and R. Car, *J. Phys.: Condens. Matter*, 2008, **20**, 083203.
16 G. Stefanucci and C.-O. Almbladh, *Europhys. Lett.*, 2004, **67**, 14.
17 G. Stefanucci and C.-O. Almbladh, *Phys. Rev. B: Condens. Matter Mater. Phys.*, 2004, **69**, 195318.
18 A. Dhar and D. Sen, *Phys. Rev. B: Condens. Matter Mater. Phys.*, 2006, **73**, 085119.
19 G. Stefanucci, *Phys. Rev. B: Condens. Matter Mater. Phys.*, 2007, **75**, 195115.
20 E. Khosravi, S. Kurth, G. Stefanucci and E. K. U. Gross, *Appl. Phys. A: Mater. Sci. Process.*, 2008, **93**, 355.
21 S. Kurth, G. Stefanucci, C.-O. Almbladh, A. Rubio and E. K. U. Gross, *Phys. Rev. B: Condens. Matter Mater. Phys.*, 2005, **72**, 035308.
22 S.-H. Ke, H. Baranger and W. Yang, *Phys. Rev. B: Condens. Matter Mater. Phys.*, 2004, **70**, 085410.
23 R. Li, J. Zhang, S. Hou, Z. Qian, Z. Shen, X. Zhao and Z. Xue, *Chem. Phys.*, 2007, **336**, 127.

